The $\Xi(1620)$ and $\Xi(1690)$ molecular states from meson-baryon interaction up to next-to-leading order

V.K. Magas([1])([2])([*]), V. Valcarce Cadenas([1])and A. Feijoo([3])

([1]) *Departament de Física Quàntica i Astrofísica, Universitat de Barcelona, Martí Franquès 1, 08028 Barcelona, Spain*

([2]) *Institut de Ciències del Cosmos, Universitat de Barcelona, Martí Franquès 1, 08028 Barcelona, Spain*

([3]) *Departamento de Física Teórica and IFIC, Centro Mixto Universidad de Valencia-CSIC, Institutos de Investigación de Paterna, Aptdo. 22085, 46071 Valencia, Spain*

Summary. — We study s-wave meson-baryon interactions with strangeness $S = -2$ in a coupled-channels chiral approach incorporating not only the leading Weinberg-Tomozawa term in the Lagrangian, but also the Born terms and next-to-leading order contributions. Our model is fitted to the experimental data set of the nonleptonic $\Xi_c^+ \to \pi^+\pi^+\Xi^-$ weak decay from the Belle Collaboration, where the $\Xi(1620)$ and $\Xi(1690)$ states were observed in their decay to $\pi^+\Xi^-$. We calculate the invariant mass distribution of the $\pi^+\Xi^-$ final state, showing that our theoretical prediction is capable of explaining the experimental data by reproducing the two resonance peaks. Regarding the pole content, we are able to dynamically generate two poles not far away from the known experimental values of the $\Xi(1620)$ and $\Xi(1690)$ states. In our approach these resonances have a molecular nature, where the lowest one strongly couples to the $\pi\Xi$ channels, while the second pole couples more strongly to the $\bar{K}\Sigma$ channels.

1. – Introduction

In the last years the experimental collaborations, such as LHCb, BABAR or Belle, have made a significant and successful contribution to the field of Hadronic Physics. Quantum numbers of various nucleons and hyperon resonances with strangeness $S = -1$ have been successfully measured. On the other hand, the number of observed hyperon resonances with $S = -2$ (Ξ states) is notably smaller at the moment. This draws our attention to the $\Xi(1620)$ and $\Xi(1690)$ states, the true nature of which has yet to be verified. According to the Particle Data Group (PDG) [1], they are assigned a status of one and three stars, respectively. Both are identified with an isospin of $I = 1/2$, forming

([*]) vladimir@fqa.ub.edu

the $\Xi^0(uss)$ and $\Xi^-(dss)$ doublet. However, their spin and parity (J^P) remain unknown, although several theoretical and experimental studies point to a value of $J^P = 1/2^-$.

The experimental evidence for the $\Xi(1620)$ is limited. In the 1970s, weak signals were reported in the $\pi\Xi$ channel of K^-p interactions [2, 3, 4], however these were accompanied by large statistical uncertainties. Finally, in 2019 Belle collaboration has determined its mass and width in its decay to $\pi^+\Xi^-$ via the $\Xi_c^+ \to \pi^+\pi^+\Xi^-$ process [5]:

$$(1)\quad M = 1610.4 \pm 6.0\ (\text{stat})^{+6.1}_{-4.2}\ (\text{syst})\ \text{MeV}\ ,\quad \Gamma = 59.9 \pm 4.8\ (\text{stat})^{+2.8}_{-7.1}\ (\text{syst})\ \text{MeV}\ .$$

The understanding of the $\Xi(1690)$ has improved over time with various experimental observations. Historically, this state was initially discovered as a threshold enhancement in the mass spectra of neutral and negatively charged $\bar{K}\Sigma$ particles in the $K^-p \to (\bar{K}\Sigma)K\pi$ reaction [6]. Subsequently, this resonance was observed in interactions between hyperons and nucleons [7, 8, 9], as well as in decays of charm baryons [10, 11, 12, 13]. In a recent experiment studying the $\Xi_b^- \to J/\psi K^-\Lambda$ decay by the LHCb Collaboration, the presence of the excited state $\Xi(1690)^-$ was confirmed [14], identifying its mass and width with high precision:

$$(2)\quad M = 1692.0 \pm 1.3\ (\text{stat})^{+1.2}_{-0.4}\ (\text{syst})\ \text{MeV}\ ,\quad \Gamma = 25.9 \pm 9.5\ (\text{stat})^{+14.0}_{-13.5}\ (\text{syst})\ \text{MeV}\ .$$

On the theoretical side, the nature of the $\Xi(1620)$ and $\Xi(1690)$ states is still a subject of ongoing debate and controversy. There are certain indications pointing to the fact that these resonances may have a nontrivial internal structure rather than a plain qqq configuration. The unavoidable analogy between $\Xi(1620)$ and $\Lambda(1405)$([1]), as its counterpart in S = -1, leads one to interpret the $\Xi(1620)$ as a molecular state arising from UχPT scheme. On this theoretical line, in Ref. [15], the authors dynamically generate the $\Xi(1620)$ resonance but with a relatively large decay width. The results of the study showed a strong coupling of the resonance to the $\pi\Xi$ and $\bar{K}\Lambda$ channels, supporting its assignment to $J^P = 1/2^-$. More recently, in Ref. [16], at the expense of reducing unnaturally one of the parameters present in the unitarization method, the $\Xi(1620)$ was pinned down to the experimental value.

On the other hand, the $\Xi(1690)$ state shows a rather strange branching ratio $\Gamma_{\pi\Xi}/\Gamma_{\bar{K}\Sigma}$ [1]. Surprisingly, despite the larger phase space that $\pi\Xi$ has compared to $\bar{K}\Sigma$, this ratio is found to be less tan 0.09. This fact finds a natural explanation when the $\Xi(1690)$ is interpreted as a meson-baryon molecule coupling strongly to the $\bar{K}\Sigma$ and $\eta\Xi$ channels, while exhibiting negligible couplings to the $\pi\Xi$ one [17, 18].

Furthermore, there exists a mutual incompatibility in pinning down both masses of dynamically generated $\Xi(1620)$ and $\Xi(1690)$ states when using a plain Weinberg-Tomozawa (WT) contact term in the Lagrangian. Only in recent work of Ref. [18] the authors incorporated to the meson-baryon interaction in the neutral $S = -2$ sector, in addition to WT term, the s-,u-channel Born terms and the tree level next-to-leading order (NLO) contribution, by adapting the BCN model (WT+Born+NLO model in Ref. [19]). And they showed that such an extended model is able to generate dynamically both $\Xi(1620)$ and $\Xi(1690)$ states in a fair agreement with the PDG compilation.

Following the recent observation of both $\Xi(1620)$ and $\Xi(1690)$ states in the $\Xi_c^+ \to \pi^+\pi^+\Xi^-$ decay by the Belle Collaboration [5], we have decided to extend and adopt the

([1]) Since 2021, the molecular nature of the $\Lambda(1405)$ has been recognized and noted in the PDG.

model of [18] to explain these experimental data. This study is still in progress [20], but some preliminary results will be published in these Proceedings. Similar attemp has been recently performed in Ref. [21], but with a model limited to WT contribution.

2. – The $\Xi_c^+ \to \pi^+\pi^+\Xi^-$ decay model

At the quark level, the Wqq' vertices accounting for $q \to q'$ weak transition are determined by the different Cabibbo-Kobayashi-Maskawa (CKM) matrix elements [22]. The dominant CKM diagram for the Ξ_c^+ decay, when a high-momentum π^+ emission is required, is depicted in Fig. 1. We can see the W-exchange weak process transforming the c quark into $su\bar{d}$, where a π^+ particle and a sus quark state are formed. This mechanism is preferred due to its favourable colour recombination factor for the outgoing quarks in the W boson, in which all the colours are allowed. Moreover, the kinematics also favour this unique quark-line diagram since we are interested in situations where the outgoing meson-baryon pair occurs at low invariant masses, which requires the emission of a high momentum π^+ [5].

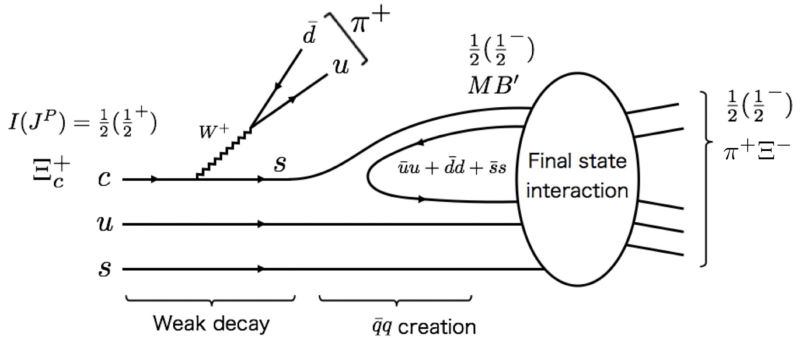

Fig. 1. – External emission diagram for the $\Xi_c^+ \to \pi^+\pi^+\Xi^-$ decay. The full (serrated) lines correspond to quarks (the W boson).

The next step is the hadronization of the sus cluster formed after the charm quark decay by introducing a vacuum-quantum-numbers $\bar{q}q$ pair from the Fermi sea, $\bar{u}u+\bar{d}d+\bar{s}s$, to construct the intermediate meson-baryon state MB'. Assuming ground states and a relative s-wave ($L = 0$) for the final $\pi^+\Xi^-$ pair, with quantum numbers $\pi^+(0^-)$ and $\Xi^-(1/2^+)$, the original sus quark state must have $J^P = 1/2^-$. Since all the quarks have $J^P = 1/2^+$, one of them, the s quark originated in the weak decay, must interact with the pair of spectarors (us, see Fig. 1) in P wave. Thus this s quark must actively participate in the hadronization process, i.e. interact with $\bar{q}q$ pair from the Fermi sea, to reach the ground state of the final system ($L = 0$).

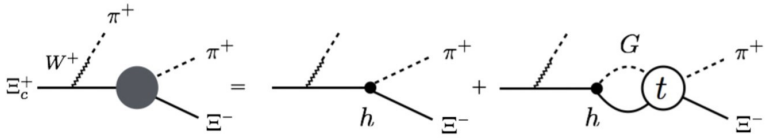

Fig. 2. – Schematic diagram of the decay amplitude for $\Xi_c^+ \to \pi^+\pi^+\Xi^-$. The first term in the right-hand side stands for the tree-level contributions, whereas the second one contains the meson-baryon loop function G involving the intermediate meson-baryon states along with their associated weights h, and the scattering amplitude t.

Following Refs. [19, 23] we can obtain the following weights for the intermediate

states:

$$|MB'\rangle = |K^-\Sigma^+\rangle - \frac{1}{\sqrt{2}}|\bar{K}^0\Sigma^0\rangle + \frac{1}{\sqrt{6}}|\bar{K}^0\Lambda\rangle - \frac{1}{\sqrt{3}}|\eta\Xi^0\rangle \quad , \tag{3}$$

where the coefficients preceding each possible state are their corresponding weights, h_i. As we can see, a direct production of the $\pi\Xi$ pairs is not possible (since the s quark originated after the weak decay should form part of the intermediate meson). However, this channel will be present in the final interaction through intermediate loops, as will be explained below.

After the production of the intermediate MB' pair, it re-scatters into the final $\pi^+\Xi^-$ state, which is parametrized by the decay amplitude $\mathcal{M}_{\pi^+\Xi^-}$. The diagrammatic representation is depicted in Fig. 2, where the total contribution is the sum of the direct tree-level process (i.e., the final state is directly produced from the $q\bar{q}$ creation) and the final-state interaction contribution of the intermediate meson-baryon pairs:

$$\mathcal{M}_{\pi^+\Xi^-}(M_{\rm inv}) = V_P \left(h_{\pi^+\Xi^-} + \sum_i h_i G_i(M_{\rm inv}) t_{i,\pi^+\Xi^-}(M_{\rm inv}) \right) \quad , \tag{4}$$

where the loop function G_i accounts for all of the possible intermediate states with its corresponding weight h_i (see Eq. (3)), whose interaction will produce the final $\pi^+\Xi^-$ pair described through the scattering amplitude $t_{i,\pi^+\Xi^-}$. All the details of the loop function and scattering amplitude calculations can be found in [18]. $M_{\rm inv}$ is the invariant mass of the meson-baryon system in the final state and V_P is a factor that incorporates the probability of the initial weak decay process as well the hadronization process. However, in the present study, following Ref. [19, 23], V_P will be taken as a constant, assuming its smooth behavior at the corresponding energy window.

In the available range of $\pi^+\Xi^-$ invariant masses produced in this experiment we also find the $\Xi(1530)$, which decays into this pair. This particular resonance is widely known in the PDG compilation [1] with a four-star rating and an average width of $\Gamma = 9.1 \pm 0.5$ MeV. It has been observed in the $\Lambda^+ \to K^+\pi^+\Xi^-$ decay, allowing us to assign a value of $I(J^P) = 1/2(3/2^+)$ to this excited state. Furthermore, the experimental data from Belle Collaboration [5] confirms the prominent signal of this resonance in our decay process of interest, $\Xi_c^+ \to \pi^+\pi^+\Xi^-$. Since our model cannot account for resonances with quantum numbers $J^P = 3/2^+$, we will explore the possibility of explicitly including the contribution of the $\Xi(1530)$ state in the final amplitude using a Breit-Wigner form:

$$\begin{aligned} \mathcal{M}_{\pi^+\Xi^-}(M_{\rm inv}) =& V_P \Bigg(h_{\pi^+\Xi^-} + \sum_i h_i G_i(M_{\rm inv}) t_{i,\pi^+\Xi^-}(M_{\rm inv}) \\ &+ \alpha \frac{M_{\Xi^*(1530)}}{M_{\rm inv} - M_{\Xi^*(1530)} + i\frac{\Gamma_{\Xi^*(1530)}}{2}} \Bigg) \quad , \end{aligned} \tag{5}$$

where the complex parameter α determines the relative weight of the $\Xi(1530)$ contribution.

With the above decay amplitude, we can calculate the invariant mass distribution

$$\frac{d\Gamma_{\pi^+\Xi^-}}{dM_{\rm inv}} = \frac{1}{(2\pi)^3} \frac{q_{\pi_H^+} q_{\pi_L^+} M_{\Xi^-}}{M_{\Xi_c^+}} |\mathcal{M}_{\pi^+\Xi^-}|^2 \,, \tag{6}$$

with $q_{\pi_H^+}$, $q_{\pi_L^+}$ being, respectively, the three-momentum of the π^+ emitted in the weak decay part in the Ξ_c^+ rest frame and the three-momentum of the meson in the final $\pi^+\Xi^-$ state in the $\pi^+\Xi^-$ rest frame. It is important to mention that the final $M_{\rm inv}$ distribution corresponds to the π^+ with the lower momentum, π_L^+ [5].

3. – Results and discussion

This work can be seen as an attempt to improve our model used in Ref. [18], which is actually an extension of the the WT+Born+NLO model of Ref. [19]. Simulation of the $\Xi_c^+ \to \pi^+\pi^+\Xi^-$ decay, measured at [5], offers us a good opportunity to extract information about the main parameters of the BCN model by fitting experimental data with MINUIT.

For the initialization of MINUIT, it is required to set input values for the parameters, as well as limits to prevent them from taking unphysical values. As a starting point, in all the fits we use the values established in Model 2 of our previous work [18] (see the first column of Table I).

There are the following 17 free parameters in the model (see [19, 18, 20]):
1-3) The factor V_p (original weak decay probability) and the $\Re\,\alpha + i\Im\,\alpha$ parameters (relative weight of the Ξ(1530) resonant mechanism). These 3 parameters are specific of the $\Xi_c^+ \to \pi^+\pi^+\Xi^-$ decay model and have no restrictions in our fits.
4-7) The 4 subtraction constants $a_{\pi\Xi}, a_{\bar{K}\Lambda}, a_{\bar{K}\Sigma}, a_{\eta\Xi}$, which are expected to be approximately of the so-called "natural size" (~ -2.0) [19], and are constrained in our fits to the range of $[-4.0, -1.0]$.
8-17) These are the main BCN model parameters: the meson decay constant f, the axial vector couplings D and F, the NLO (in chiral Lagrangian) parameters $b_0, b_D, b_F, d_1, d_2, d_3$, d_4. In order to be consistent with previously obtained results, we would like these parameters to stay as close as possible to their original values from [19]. In that paper, the authors, after performing a dedicated study, present not only nominal parameter values but also associated uncertainties - the standart deviations, σ, for all the model parameters can be found in the first column of Table I.

Based on this information we perform three consequent fits, when the main BCN model parameters are restricted within 1σ range around their nominal values, **Model A**; restricted within 2σ range - **Model B**; without any limits - **Model C**. The obtained results are displayed in the corresponding columns of Table I and shown in Fig. 3.

Model A. The permition of 1σ variation of the main model parameters leads to a fair agreement with experimental data, as we can see in Fig. 3. This new parametrization moves substracting constants towards their natural size. However, all the main BCN parameters approach their limiting values. This observation motivated us to continue our study by increasing the possible range of parameters variation.

The decay constant f tends towards its upper maximum, while the axial vector couplings move towards their lowest error bars, resulting in a significant discrepancy in their sum compared to the reference value of $g_A = D + F = 1.26 \pm 0.05$. Nevertheless, the final $\chi^2_{\rm d.o.f} = 1.99$ is not far from unity, indicating a high level of overall agreement with the experimental data, as can be seen in Fig. 3. One can clearly observe the two peaks corresponding to the Ξ(1620) and Ξ(1690) resonances, as well as the explicit inclusion of the Ξ(1530) resonant term with $J^P = 3/2^+$.

Model B. To further explore the capabilities of the model, we can extend the variation ranges of the main BCN model parameters up to 2σ. Such a fit produces

	Model 2 (from [18])	Model A (1σ)	Model B (2σ)	Model C (no limits)
$a_{\pi\Xi}$	-2.7228	$-2.6703 \pm 6 \cdot 10^{-6}$	-2.6887 ± 0.0713	$-1.2302 \pm 8 \cdot 10^{-6}$
$a_{\bar{K}\Lambda}$	-1.0000	$-1.8658 \pm 3 \cdot 10^{-6}$	-2.0873 ± 0.1212	$-1.4011 \pm 3 \cdot 10^{-6}$
$a_{\bar{K}\Sigma}$	-2.9381	$-1.3112 \pm 3 \cdot 10^{-6}$	-1.4821 ± 0.0252	$-2.9452 \pm 5 \cdot 10^{-6}$
$a_{\eta\Xi}$	-3.3984	$-2.2348 \pm 7 \cdot 10^{-6}$	-2.2220 ± 0.1054	$-2.1954 \pm 4 \cdot 10^{-6}$
f/f_π	$1.204^{+0.005}_{-0.015}$	$1.209 \pm 4 \cdot 10^{-10}$	1.222 ± 0.005	$1.2297 \pm 2 \cdot 10^{-6}$
b_0 [GeV^{-1}]	$0.129^{+0.032}_{-0.032}$	$0.161 \pm 4 \cdot 10^{-9}$	0.193 ± 0.012	$0.410 \pm 3 \cdot 10^{-6}$
b_D [GeV^{-1}]	$0.120^{+0.010}_{-0.09}$	$0.130 \pm 10 \cdot 10^{-10}$	0.140 ± 0.004	$-0.059 \pm 6 \cdot 10^{-6}$
b_F [GeV^{-1}]	$0.209^{+0.022}_{-0.026}$	$0.231 \pm 7 \cdot 10^{-8}$	0.253 ± 0.013	$1.061 \pm 6 \cdot 10^{-6}$
d_1 [GeV^{-1}]	$0.151^{+0.021}_{-0.027}$	$0.124 \pm 7 \cdot 10^{-10}$	0.097 ± 0.005	$-1.903 \pm 6 \cdot 10^{-6}$
d_2 [GeV^{-1}]	$0.126^{+0.012}_{-0.009}$	$0.117 \pm 2 \cdot 10^{-10}$	0.108 ± 0.001	$1.333 \pm 1 \cdot 10^{-5}$
d_3 [GeV^{-1}]	$0.299^{+0.020}_{-0.024}$	$0.275 \pm 3 \cdot 10^{-7}$	0.251 ± 0.073	$-0.944 \pm 5 \cdot 10^{-5}$
d_4 [GeV^{-1}]	$0.249^{+0.027}_{-0.033}$	$0.216 \pm 1 \cdot 10^{-9}$	0.183 ± 0.006	$-0.837 \pm 7 \cdot 10^{-6}$
D	$0.700^{+0.064}_{-0.144}$	$0.556 \pm 4 \cdot 10^{-8}$	0.589 ± 0.031	$0.654 \pm 9 \cdot 10^{-6}$
F	$0.510^{+0.060}_{-0.050}$	$0.460 \pm 3 \cdot 10^{-9}$	0.421 ± 0.030	$0.550 \pm 3 \cdot 10^{-6}$
V_P [MeV^{-1}]	-	3.9137 ± 0.0002	3.7773 ± 0.1927	3.1330 ± 0.0003
$Re(\alpha)(\times 10^{-3})$	-	$0.3597 \pm 1 \cdot 10^{-5}$	0.4265 ± 0.0366	$2.3448 \pm 3 \cdot 10^{-6}$
$Im(\alpha)$	-	$-0.2488 \pm 1 \cdot 10^{-10}$	$-0.2249 \pm 5 \cdot 10^{-8}$	$-0.0399 \pm 6 \cdot 10^{-10}$
$\chi^2_{\text{d.o.f.}}$	-	1.99	1.44	0.72

TABLE I. – *Values of the free parameters and the corresponding $\chi^2_{d.o.f.}$ for the different fits described in the text. The subtraction constants are taken at a regularization scale $\mu = 630$ MeV [19, 18] and the value of the pion decay constant is $f_\pi = 93$ MeV. The error bars in the parameters of Models A,B and C are directly provided by the MINUIT minimization procedure.*

$\chi^2_{\text{d.o.f}} = 1.44$, indicating a better matching the experimental data with respect to Model A, as can be seen in Fig. 3. The new parametrization exhibits a trend, where the parameters move towards the limits, following the same direction as in Model A.

Model C. As a final test, we decided to remove the limits for the main model parameters, and the performed fit reaches the best agreement with experimental data (see Fig. 3) and exhibits the smallest $\chi^2_{\text{d.o.f}}$ value, specifically 0.72 (see Table I). The price to pay, however, is that some of the parameters have changed by an order of magnitud, see for example d_1 and d_2. Although the exact limits of these parameters are not known, still in most of the fits they get values close to those of Models A and B [24]. This is one of the reasons why we can not consider Model C as the best one.

On the other hand, the obtained $\chi^2_{\text{d.o.f}}$ substantially less than 1, characterizes an overly satisfactory fit. And, thus, our entire analysis reveals a lack of sufficient data to determine our adjustable parameters in an unambiguous manner.

At the moment, we shall consider Model A as our best fit, because it is capable of describing the experimental Ξ_c^+ spectrum by generating the two resonances, potentially

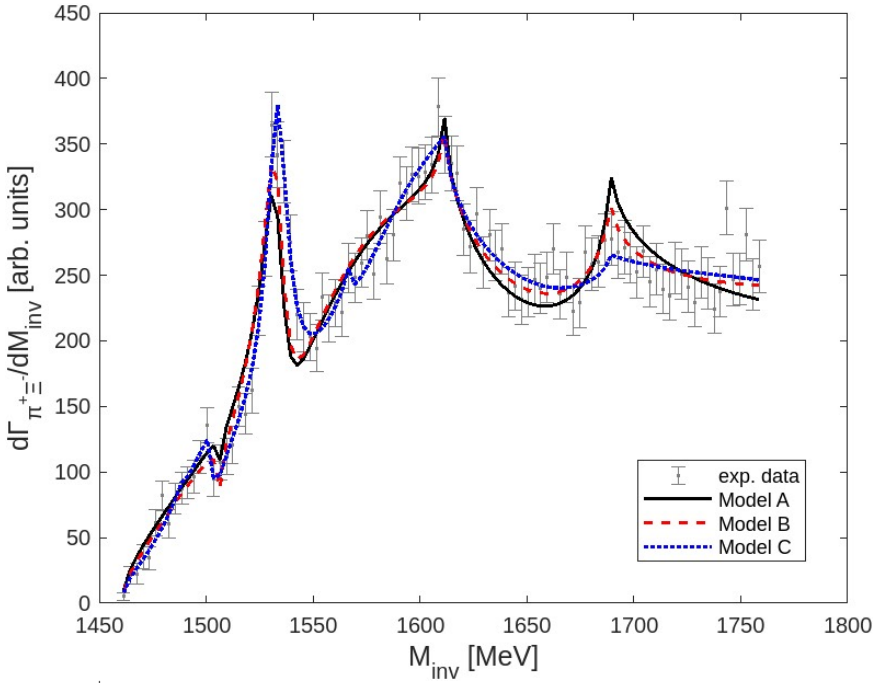

Fig. 3. – The $\pi^+\Xi^-$ invariant mass distribution obtained with Model A (solid black line), Model B (dashed red line) and Model C (dotted blue line). The experimental data (points with errorbars) provided by the Belle Collaboration [5].

associated with Ξ(1620) and Ξ(1690), based on values of the main model parameters that fall within a 1σ error range from the values determined in the $S = -1$ sector in Ref. [19]. This implies that we are operating within the physical validity of $SU(3)$ symmetry. Additionally, as it can be seen in Table I, we observe that the minimum of Model A is very sharp, since the uncertainties for all the parameters in the model, as estimated by MINUIT, are extremely small, in contrast to, for example, Model B.

With this new parametrization, Model A, we can now search for poles in the second Riemann sheet of the scattering amplitude. The results revealed the presence of two poles: $z_1 = 1571.33 - i71.99$ MeV and $z_2 = 1707.00 - i207.92$ MeV, which, however, have moved rather far from the positions of resonances generated in [18]: $z_1' = 1608.51 - i85$ MeV and $z_2' = 1686.17 - i14.86$. We also find that the lowest (highest) energy one strongly couples to $\pi\Xi$ and $\bar{K}\Lambda$ ($K\Sigma$ and $\eta\Xi$) states, what allows us to associate them with the Ξ(1620) and Ξ(1690) resonances. The much broader width of the second pole is attributed to the opening of the $\bar{K}^0\Sigma^0$ channel, to which it couples strongly.

The Belle Collaboration, analyzing the same data [5], has obtained rather different information about the Ξ(1620) pole, as seen in Eq. (1). This difference is related to the type of analysis performed. In particular, they modeled the signal of the resonances using a Breit-Wigner function [5]. However, our peaks (see Fig. 3) exhibit a distorted shape with an effective reduction in width compared to the theoretical values due to the Flatté effect [25]. This well-known effect occurs when a resonance is located close enough (in terms of its width) to the channel threshold whose coupling to this structure is strong. The opening of the $\bar{K}^0\Lambda$ channel near the z_1 pole results in an experimental width around 60 MeV, in agreement with the value compiled by the PDG. The same effect is observed for the z_2 pole, which exhibits a rather narrow resonance width of around 40 MeV.

In summary, the UχPT scheme, taking into account higher order contributions, is able to explain with sufficient accuracy the observed $M_{\pi^+\Xi^-}$ spectrum [5] and reproduce the $\Xi(1620)$ and $\Xi(1690)$ molecular states. However, to completely determine all the model parameters we would need more experimental data in this sector. A recent analysis of the $K^-\Lambda$ correlation function by the ALICE Collaboration [26] could potentially help us to resolve this situation. According to Ref. [27], the inclusion of these new data may change our ideas about which interaction channels are responsible for the generation of $\Xi(1620)$ and $\Xi(1690)$. This will be the next step in our research.

* * *

This work was supported by the Ministerio de Ciencia e Innovación of Spain through the "Unit of Excellence María de Maeztu 2020-2023" award to the Institute of Cosmos Sciences (CEX2019-000918-M) and under the projects PID2020-118758GB-I00 and PID2020-112777GB-I00, and by Generalitat Valenciana under contract PROMETEO/ 2020/023. This project has received funding from the European Union Horizon 2020 research and innovation programme under the program H2020-INFRAIA-2018-1, grant agreement No. 824093 of the STRONG-2020 project. The work of A. F. was partially supported by the Generalitat Valenciana and European Social Fund APOSTD-2021-112.

REFERENCES

[1] Workman R.L. *et al.* [Particle Data Group], *PTEP*, **2022** (2022) 083C01.
[2] Ross R. T. *et al.*, *Phys. Lett. B*, **38** (1972) 177.
[3] de Bellefon A. *et al.*, *Nuovo Cimento*, **28** (1975) 289.
[4] Briefel E. *et al.*, *Phys. Rev. D*, **16** (1977) 2706.
[5] Sumihama M. *et al.*, *Phys. Rev. Lett.*, **122** (2019) 072501.
[6] Dionisi C. *et al.* [Amsterdam-CERN-Nijmegen-Oxford], *Phys. Lett. B*, **80** (1978) 145.
[7] Biagi S. F. *et al.*, *Z. Phys. C*, **9** (1981) 305.
[8] Biagi S. F. *et al.*, *Z. Phys. C*, **34** (1987) 15.
[9] Adamovich M. I. *et al.* [WA89], *Eur. Phys. J. C*, **5** (1998) 621.
[10] Abe K. *et al.* [Belle], *Phys. Lett. B*, **524** (2002) 33.
[11] Link J. M. *et al.* [FOCUS], *Phys. Lett. B*, **624** (2005) 22.
[12] Aubert B. *et al.* [BaBar], *Phys. Rev. D*, **78** (2008) 034008.
[13] Ablikim M. *et al.* [BESIII], *Phys. Rev. D*, **92** (2015) 092006.
[14] Aaij R. *et al.*, *Sci. Bull.*, **66** (2021) 1278.
[15] Ramos A. and Oset E. and Bennhold C., *Phys. Rev. Lett.*, **89** (2002) 252001.
[16] Nishibuchi T. and Hyodo T., *EPJ Web Conf.*, **271** (2022) 10002.
[17] Sekihara T., *PTEP*, **9** (2015) 091D01.
[18] Feijoo A. and Valcarce V. and Magas V.K., *Phys. Lett. B*, **841** (2023) 137927.
[19] Feijoo A. and Magas V.K. and Ramos A., *Phys. Rev. C*, **99** (2019) 035211.
[20] Valcarce V., Master's Thesis (Inter-University Master's Degree in Nuclear Physics), University of Barcelona (2023).
[21] Li Hai-Peng *et al.*, *Eur. Phys. J. C*, **83** (2023) 954.
[22] Chau L. L., *Phys. Rept.*, **95** (1983) 1.
[23] Miyahara K. *et al.*, *Phys. Rev. C*, **95** (2017) 035212.
[24] Kaiser N. and Siegel P.B.and Weise W., *Nucl. Phys. A*, **594** (1995) 325; Borasoy B. and Nissler R. and Weise W., *Eur. Phys. J. A*, **25** (2005) 79; Cieply A. and Smejkal J., *Eur. Phys. J. A*, **43** (2010) 191; Ikeda Y. and Hyodo T. and Weise W., *Nucl. Phys. A*, **881** (2012) 98.
[25] Flatté S.M., *Phys. Lett. B*, **63** (1976) 224.
[26] Acharya S. *et al.* [ALICE], *Phys. Lett. B*, **845** (2023) 138145.
[27] Sarti V.M. *et al.*, [arXiv:2309.08756 [hep-ph]].